Supporting Information

2D Conductive Metal-Organic Frameworks for NO Electrochemical Reduction: A First-Principles Study

Xing Chen, [a#] *Xiangyu Zhu,* [a#] *Zhiyuan Xia,* [a] *Shiting Qian,*[a] *Yanan Zhou* [b]* *Qiquan Luo*[a]* *and Jinlong Yang*[c]*

[a]*Institutes of Physical Science and Information Technology, Anhui University, Hefei 230601, China.*

[b]*School of Material Science and Chemical Engineering, Institute of Mass Spectrometry, Ningbo University, Fenghua Road 818, Ningbo 315211, China.*

[c]*Key Laboratory of Precision and Intelligent Chemistry, Department of Chemical Physics, Hefei National Research Center for Physical Sciences at the Microscale, University of Science and Technology of China, Hefei, Anhui 230026, China.*

#X.C and X.Z contributed equally to this work

*Email: qluo@ustc.edu.cn; zhouyanan@nbu.edu.cn; jlyang@ustc.edu.cn.

Table of content

Constant potential method.....S1
The model details for Pt(100).....S3
Nitric oxide reduction five-electron mechanism.....S4
Detailed descriptions and computational details of SISSO method.....S5
One-dimensional descriptors of TMX_4-HTPs.....S6
Fig. S1 Top view of TMX_4-HTP monolayer.....S7
Fig. S2 Three possible adsorption patterns of NO on TMX_4-HTPs.....S8
Fig. S3 The energy profile of the protonation processes for Pt(100).....S9
Fig. S4 Energy(ΔG_1) required for the first protonation step.....S10
Fig. S5 Schematic pathways of the NORR process toward NH_3 synthesis.....S11
Fig. S6 Free energy diagrams of electrochemical NO-to-NH_3.....S12
Fig. S7 Energy profile for AIMD simulation.....S13
Fig. S8 The molecular orbital diagram of NO.....S14
Fig. S9 PDOS of (a)TMN_4-HTPs, (b)TMO_4-HTPs, (c) TMP_4-HTPs, and (d)TMS_4-HTPs.....S15
Fig. S10 PDOS of NO-adsorbed (a)TMN_4-HTPs, (b)TMO_4-HTPs, (c) TMP_4-HTPs, and (d)TMS_4-HTPs.....S16
Fig. S11 Scaling relationship among free energies of NO, transfer charge of TM atoms, and the N-O bond of adsorbed NO on TMX_4-HTPs.....S17
Fig. S12 Adsorption free energies of HNO (ΔG_{*HNO}), NOH (ΔG_{*NHO}).....S18
Fig. S13 PDOS of MnO_4-HTP adsorbed with HNO and NOH.....S19
Fig. S14 The PDOS of MnO-HTP by HSE06 hybrid functional.....S20
Fig. S15 Free energy diagrams of electrochemical NO-to-NH_3 conversion on MnO_4-HTP by PBE+SOL+U.....S21
Fig. S16 Simulated polarization curve of MnO_4-HTP and Pt (100).....S22
Fig. S17 Total energies of intermediates as a function of applied potential U.....S23
Fig. S18 The free energy curves of MnO_4-HTP under varying electrode potentials at (a) pH=1, and (b) pH=13.....S24
Fig. S19 pH-dependent and potential-dependent contour plot of the reaction energy for the second protonation step.....S25
Fig. S20 The DFT-calculated ΔG_{*H}, ΔG_{*H2O} and ΔG_{*NH3} values of TMX_4-HTP were compared with the SISSO predicted values.....S26
Fig S21 Comparison of DFT-calculated ΔG_{*H}, ΔG_{*H2O} and ΔG_{*NH3} values with the SISSO-predicted values.....S27
Fig. S21 The structure of Fe–N–C.....S28
Fig. S23 Free energy diagrams of CoO_4-HTP, CuO_4-HTP, and $Co_{0.5}Cu_{0.5}O_4$-HTP.....S29
Tab. S1 Calculated energies of MnO_4-HTP at different vacuum spaces.....S30
Tab. S2 TMX_4-HTP energy and lattice length a, b.....S31
Tab. S3 Computed the μ_{TM}, E_f, U°_{diss} , N_e, U_{diss}.....S32
Tab. S4 Free energies of NO on TMX_4-HTPs with N-end, O-end, and side-on patterns.....S33
Tab. S5 Free energies of NO, H, H_2O, and NH_3 on TMX_4-HTPs.....S34
Tab. S6 Energy(ΔG_1) required for the first protonation step.....S35
Tab. S7 The energy of all the possible intermediates.....S36

Tab. S8 Transfer charge of TM atoms, and the N-O bond of adsorbed NO on TMX_4-HTPs. S40
Tab. S9 Adsorption free energies of Δ^*G_{HNO}, ΔG_{*NOH}, $\Delta G_{HNO} - \Delta G_{NOH}$ S41
Tab. S10 Q_X, N, AR, IR, IE, EA, ρ_{TM}, M, χ of each investigated TMX_4-HTPs. S42

Constant potential method

This method implements VASPsol to model the electrochemical electrode/solution interface and establish the relationship between charge and electrode potential. For each structure, thirteen different systems were performed at charges of $-2e^-$ to $+2e^-$ at a step of $0.5e^-$ and the corresponding electrode potential referenced to the SHE scale could be calculated by

$$U_q(\mathrm{V/SHE}) = (\phi_q(f) - 4.6)/e$$

where $\phi_q(f)$ is the work function of the charging system and 4.6 V is the work function of the H_2/H^+ couple under standard conditions.

Under the condition of fixed potential, the electrode potential referenced to the SHE scale is changed by pH values. The relationship is given by

$$U_{\mathrm{RHE}} = U_{\mathrm{SHE}} + k_B T \ln(10)\mathrm{pH}/e$$

Therefore, by adjusting the charge numbers of the system, the energies under specific potentials could be calculated. However, the DFT-calculated value also includes the interaction between the electrons in the slab and the background charge. It is given by

$$E_{\mathrm{DFT}}(n_e, n_{bg}) = E_{\mathrm{slab}}(n_e) + E_{\mathrm{slab-bg}}(n_e, n_{bg}) + E_{\mathrm{bg}}(n_{bg})$$

where E_{slab} is the energy of the slab without the background, E_{bg} is the energy of the background without the slab and $E_{\mathrm{slab-bg}}$ is the interaction energy between the slab and the background. According to Neurock's methods,[1] decoupling of the slab-background interaction involves subtracting the $E_{\mathrm{slab-bg}}$ and E_{bg} terms, which sum to equal $-\int_0^q \langle \bar{V}_{\mathrm{tot}}(Q) \rangle dQ$, where $\langle \bar{V}_{\mathrm{tot}}(Q) \rangle$ is the average potential in the unit cell. The $\langle \bar{V}_{\mathrm{tot}}(Q) \rangle$ is obtained from the LOCPOT file generated by VASP with LVHAR set as true. The average electrostatic potential in the x, y, and z directions provided by the LOCPOT file is summed ($\iiint V_{\mathrm{tot}} dxdydz$). $\frac{1}{\Sigma}\iiint V_{\mathrm{tot}} dxdydz$ (i.e., the potential shift to reference the system to vacuum as a function of q), and Σ is the volume of the unit cell. The correction results in the total electron energy, E_{elec}, defined as:

$$E_{elec} = E_{DFT} + \int_0^q \langle \bar{V}_{tot}(Q) \rangle dQ$$

where E_{elec} is equal to $E_{slab}(n_e)$, E_{DFT} is equal to $E_{DFT}(n_e, n_{bg})$, and $E_{slab\text{-}bg}(n_e, n_{bg}) + E_{bg}(n_{bg})$ is equal to $-\int_0^q \langle \bar{V}_{tot}(Q) \rangle dQ$. However, the total free energy of the system (E_{Free}) also includes contributions for the excess electrons (q) at the Fermi potential ($\phi_q(f)$) and is equivalent to

$$E_{free}(U) = E_{DFT} + \int_0^q \langle \bar{V}_{tot}(Q) \rangle dQ - q\phi_q(f)$$

E_{free} and U could be fitted to a quadratic function form, consistent with a capacitor created by the charged-slab/background-charge system, written as

$$E(U) = -\frac{1}{2}C(U - U_0)^2 + E_0$$

where U_0 is the potential of zero charge (PZC), E_0 is the energy at the PZC, and C is the capacitance of the surface. From the quadratic functions, the potential-dependent energy could be provided.

The model details for Pt(100)

The Pt(100) surface is represented by a 3 × 3 unit cell with five Pt layers (total of 45 atoms per unit cell). Surface relaxation is allowed in the top three layers of the (100) slab.

Nitric oxide reduction five-electron mechanism

The overall NORR process includes a five-electron mechanism, which consists of five elementary steps following the equations as reported in the previous literature:

the first protonation step	$^{*} + NO + H + e^{-} \rightarrow {}^{*}HNO({}^{*}NOH)$
the second protonation step	$^{*}HNO + H + e^{-} \rightarrow {}^{*}HNOH({}^{*}H_2NO)$ $^{*}NOH + H + e^{-} \rightarrow {}^{*}HNOH({}^{*}N + H_2O)$
the thrid protonation step	$^{*}HNOH + H + e^{-} \rightarrow {}^{*}H_2NOH({}^{*}NH + H_2O)$ $^{*}H_2NO + H + e^{-} \rightarrow {}^{*}H_2NOH({}^{*}O + NH_3)$ $^{*}N + H + e^{-} \rightarrow {}^{*}NH$
the fourth protonation step	$^{*}NH + H + e^{-} \rightarrow {}^{*}NH_2$ $^{*}H_2NOH + H + e^{-} \rightarrow {}^{*}NH_2 + H_2O$ $^{*}H_2NOH + H + e^{-} \rightarrow {}^{*}OH + NH_3$
the fifth protonation step	$^{*}NH_2 + H + e^{-} \rightarrow {}^{*}NH_3$ $^{*}OH + H + e^{-} \rightarrow {}^{*}H_2O$

where * represents the active site on the catalyst, and $^{*}HNO$, $^{*}NOH$, $^{*}HNOH$, $^{*}H_2NO$, $^{*}N$, $^{*}H_2NOH$, $^{*}O$, $^{*}NH$, $^{*}NH_2$, $^{*}OH$, $^{*}NH_3$, and $^{*}H_2O$ are the correspond adsorbed intermediates, respectively.

Detailed descriptions and computational details of SISSO method

SISSO is a data-driven method combining symbolic regression and compressed sensing to produce explicit mathematical expressions.[2, 3] The main steps of this method are: (1) uniformly sample a sufficient number of reliable data points; (2) identify key features based on domain knowledge or intuition; (3) construct a large feature space through feature transformations to better describe target properties; (4) assume that target properties can be linearly expanded in the feature space and solve for the sparse solution of the linear model. In this work, the initial feature space comprises 13 primary features Φ_0 = [Q_x, Q_{TM}, Ne, N, AR, IR, IE, EA, ρ_{TM}, M, χ, U°_{diss}, μ_{TM}], and the mathematical operations for feature construction are (+, −, ×, /, $^{-1}$, ^{2}, ^{3}, |−|, $\sqrt{\ }$, $\sqrt[3]{\ }$). With these primary features and mathematical operations, a large number of expressions are generated. The SISSO code is available at http://github.com/rouyang2017/SISSO.

One-dimensional descriptors of TMX4-HTPs

The ΔG_{*NO} is depicted as:

$$\Delta G_{*NO}\,(\mathrm{SISSO}) = -38.97 \times \frac{\mathrm{IE} \times \left(\frac{\mu_{TM}}{M}\right)^2}{Q_X \times N \times N_e} + 1.17$$

The ΔG_{*H} is depicted as:

$$\Delta G_{*H}\,(\mathrm{SISSO}) = -0.38 \times \left(\frac{(Q_X - N) \times N_e + (N - N_e) \times N}{\mu_{TM}}\right) - 2.35$$

The ΔG_{*H2O} is depicted as:

$$\Delta G_{*H2O}\,(\mathrm{SISSO}) = -0.26 \times \left(\frac{e^{N_e} \times N \times \rho_{TM} \times \ln Q_X}{N + N_e}\right) \times 10^{-1} - 3.36$$

The ΔG_{*NH3} is depicted as:

$$\Delta G_{*NH3}\,(\mathrm{SISSO}) = -1132.82 \times \frac{\mu_{TM}^2}{N \times \rho_{TM} \times \sqrt{Q_X} \times N_e \times AR} + 1.17$$

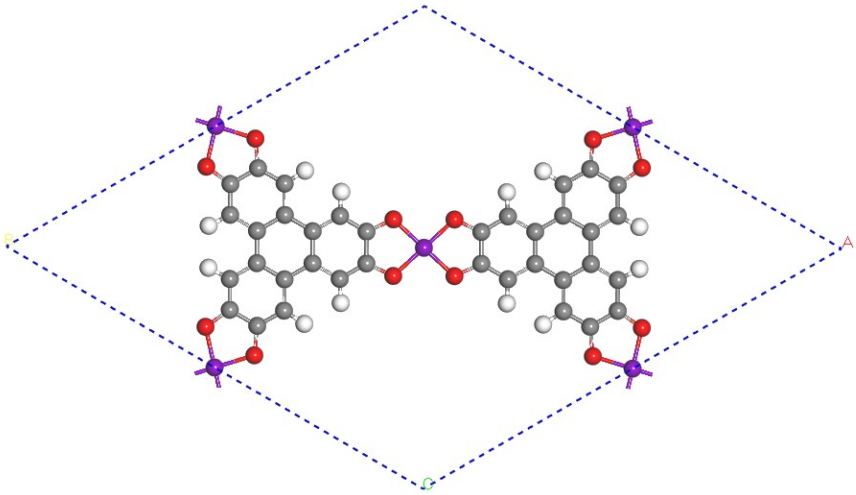

Fig. S1 Top view of TMX_4-HTP monolayer.

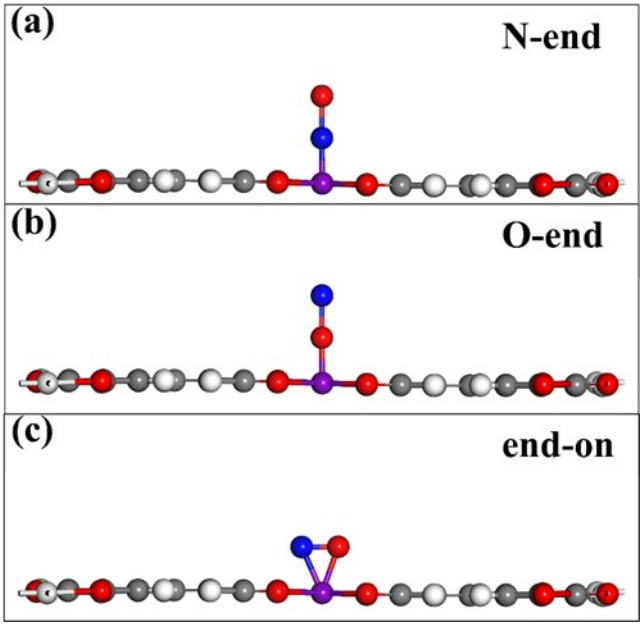

Fig. S2 Three possible adsorption patterns of NO on TMX_4-HTPs.

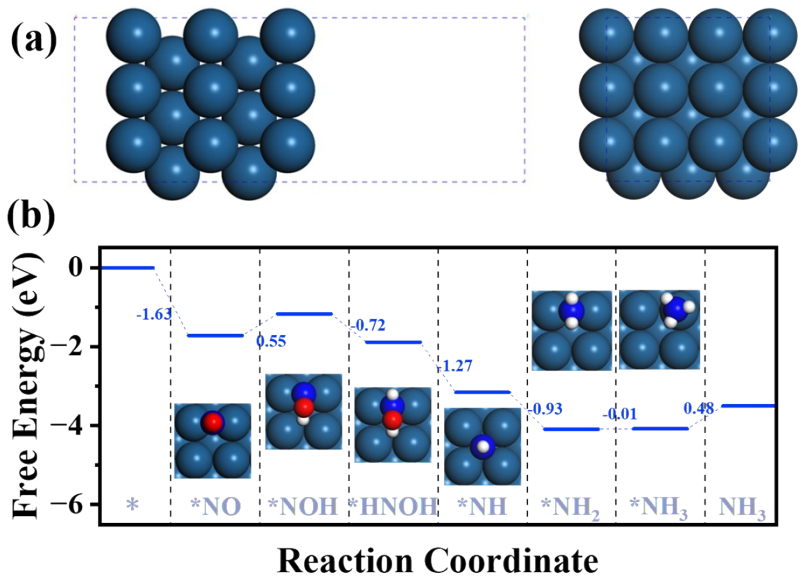

Fig. S3 (a) The side and top views of the Pt(100), (b) The energy profile of the protonation processes for Pt(100)

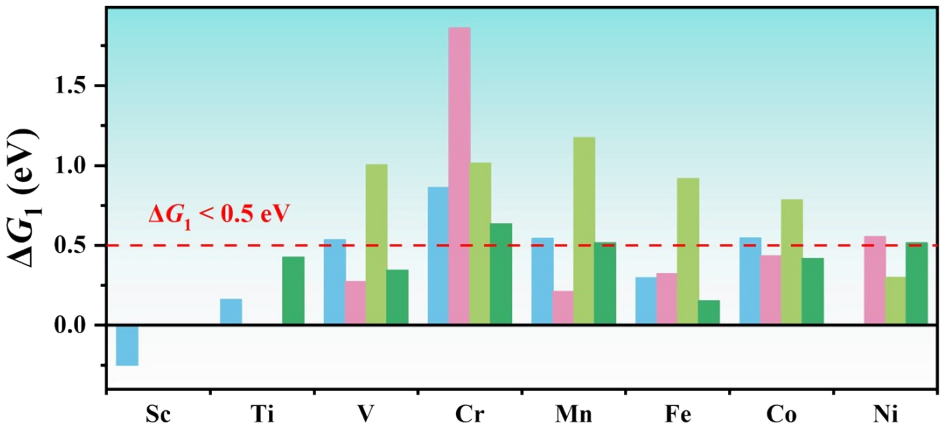

Fig. S4 Energy(ΔG_1) required for the first protonation step of NO + H^+ + e^- → HNO(NOH).

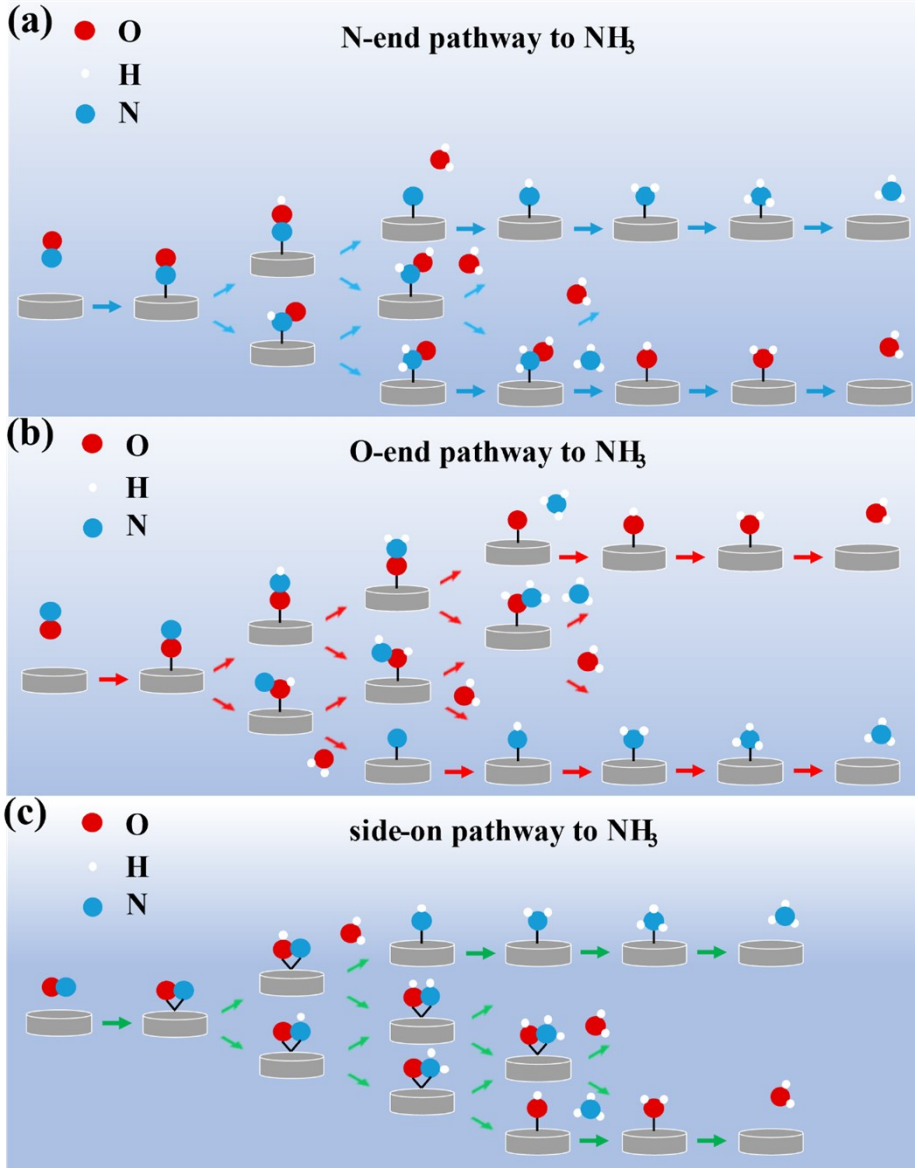

Fig. S5 Schematic pathways of the NORR process toward NH_3 synthesis.

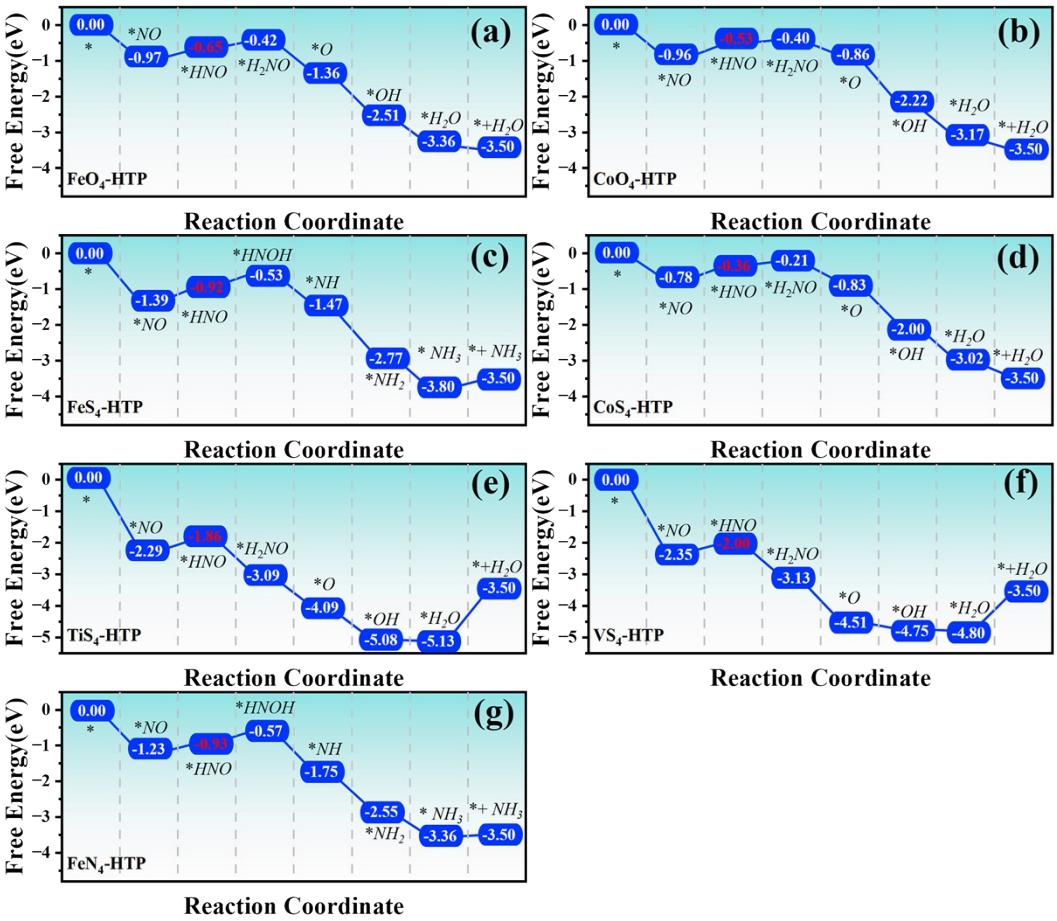

Fig. S6 Free energy diagrams of electrochemical NO-to-NH_3 conversion on (a) FeO_4-HTP, (b) CoO_4-HTP, (c)FeS_4-HTP, (d) CoS_4-HTP, (e) TiS_4-HTP, (f) VS_4-HTP, and (g) FeN_4-HTP.

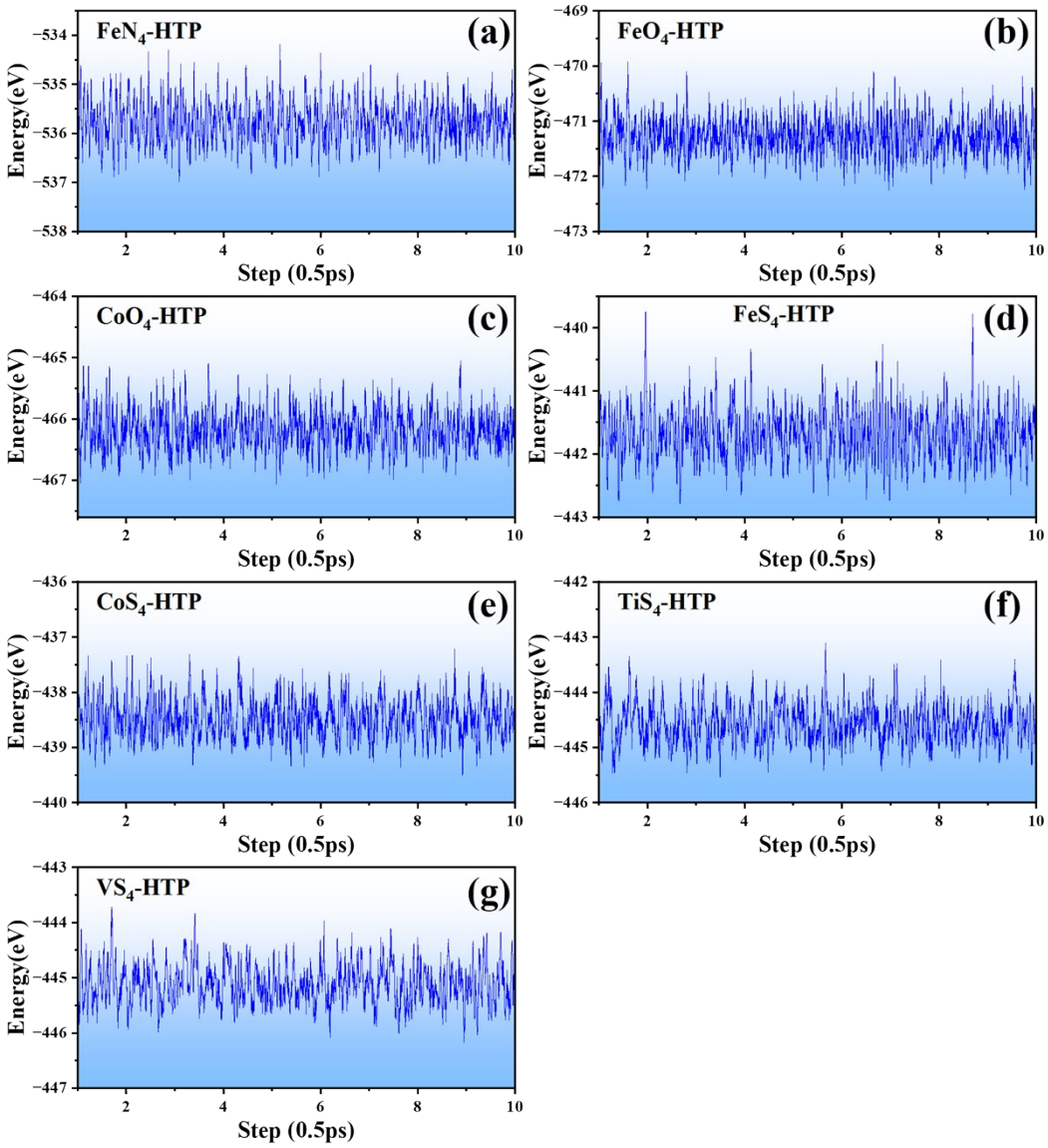

Fig. S7 Energy profile for *ab initio* molecular dynamics (AIMD) simulation on (a) FeN_4-HTP, (b) FeO_4-HTP, (c) MnO_4-HTP, (d) CoO_4-HTP, (e) FeS_4-HTP, (f) CoO_4-HTP, (g) TiS_4-HTP, and (h) VS_4-HTP after 10 ps at 350 K, where the energy fluctuation is caused by thermal disturbance of temperature.

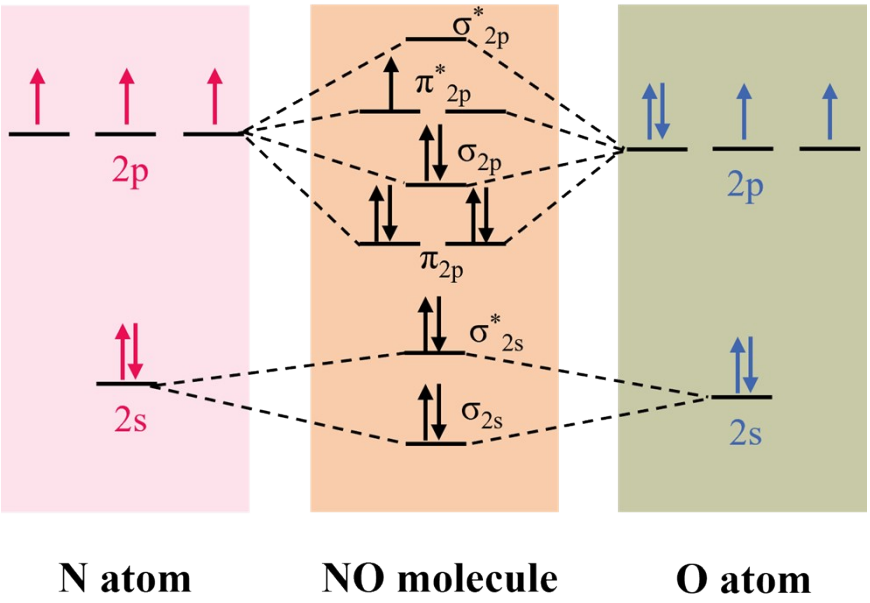

Fig. S8 The molecular orbital diagram of NO.

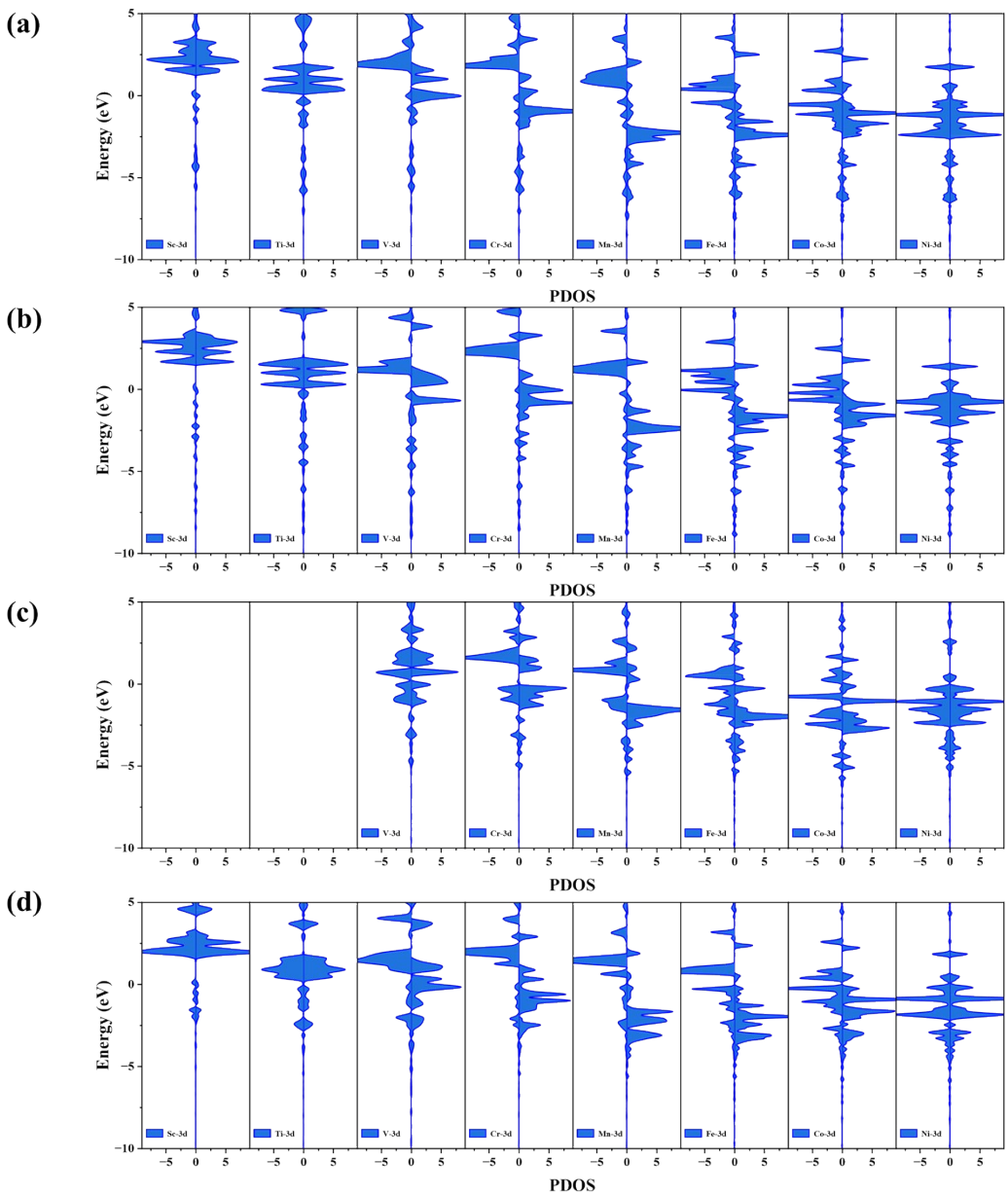

Fig. S9 Partial density of states (PDOS) of (a)TMN_4-HTPs, (b)TMO_4-HTPs, (c) TMP_4-HTPs, and (d)TMS_4-HTPs. The Fermi level is set to 0 eV.

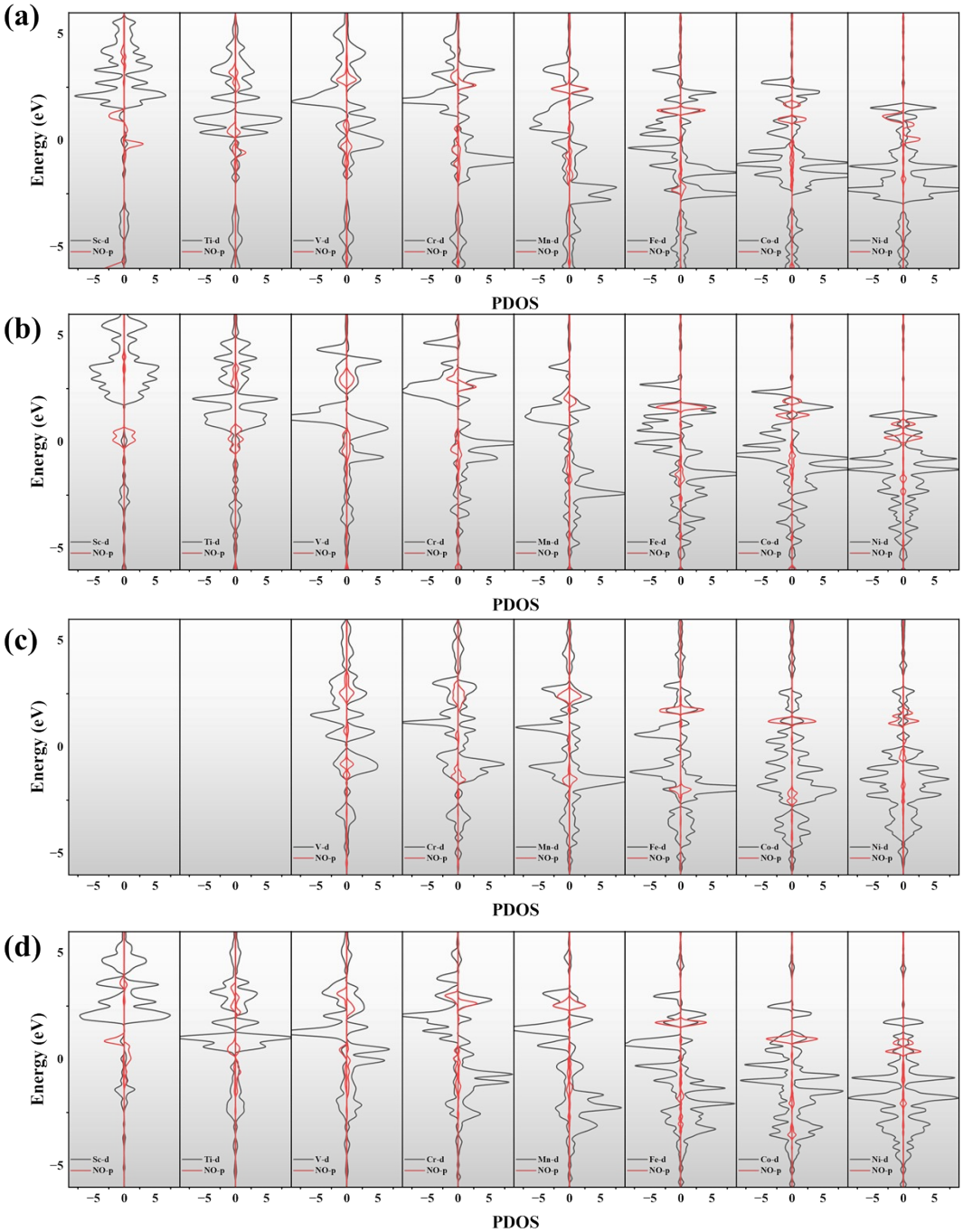

Fig. S10 PDOS of NO-adsorbed (a)TMN_4-HTPs, (b)TMO_4-HTPs, (c) TMP_4-HTPs, and (d)TMS_4-HTPs. The Fermi level is set to 0 eV.

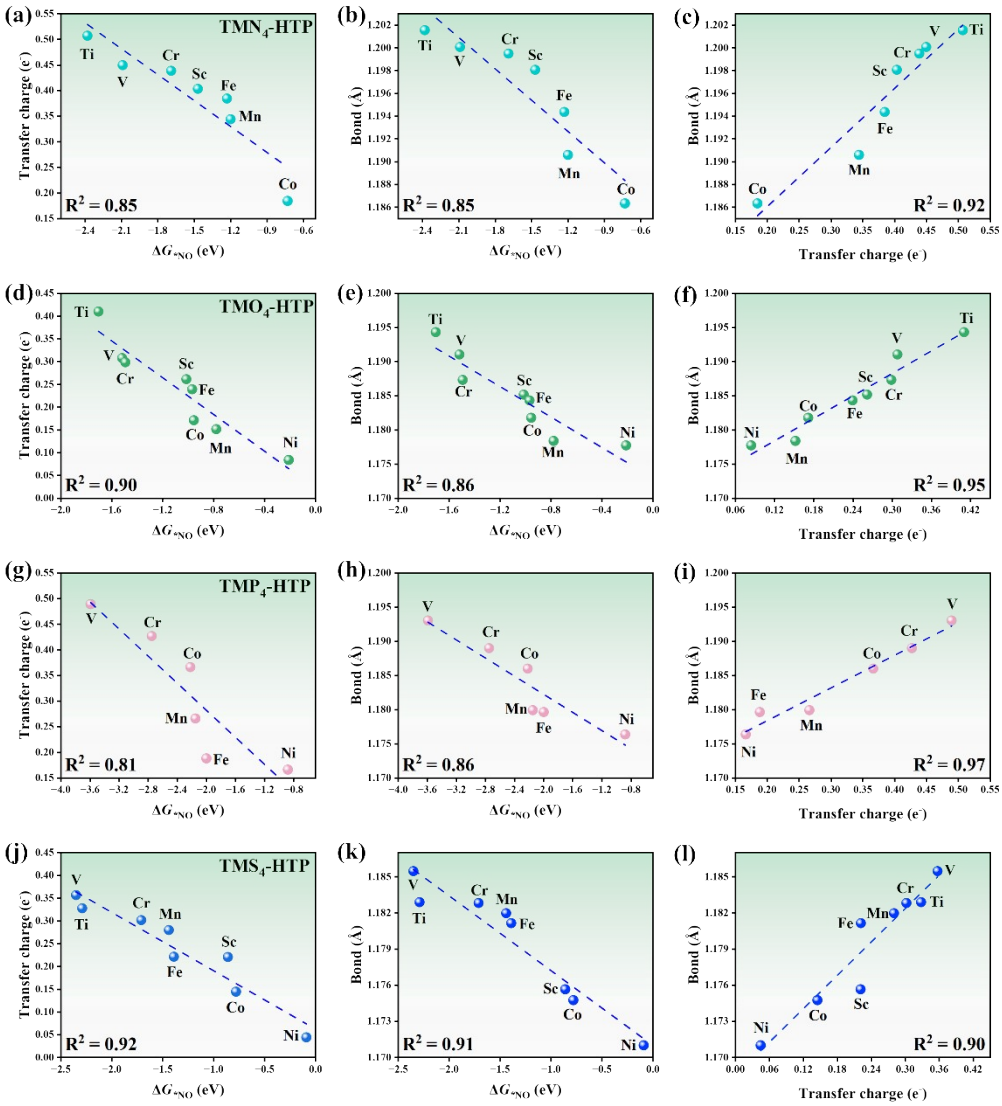

Fig. S11 Scaling relationship among free energies of NO (ΔG_{*NO}), transfer charge of TM atoms (Q_{TM}), and the N-O bond of adsorbed NO ($d_{N\text{-}O}$) on TMX_4-HTPs.

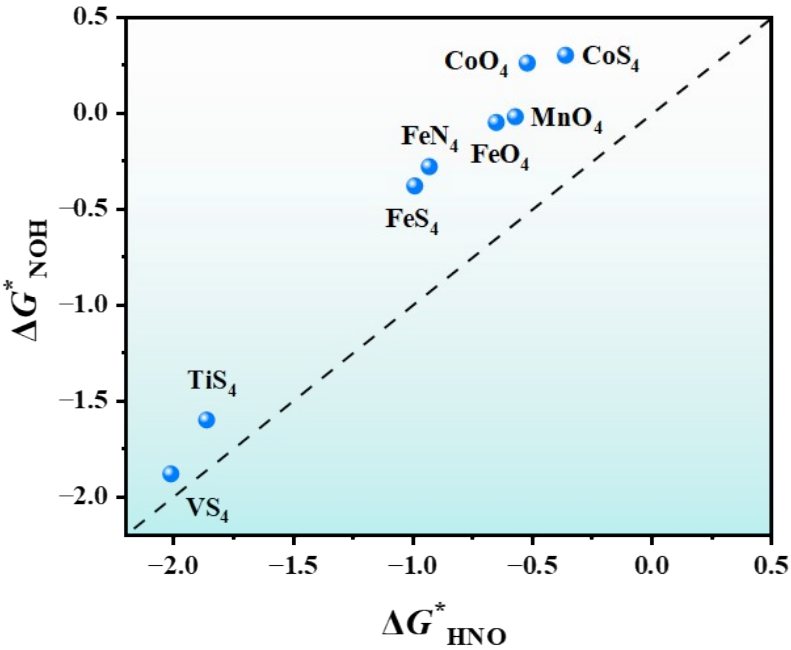

Fig. S12 Adsorption free energies of HNO (ΔG_{*HNO}), NOH (ΔG_{*NHO}).

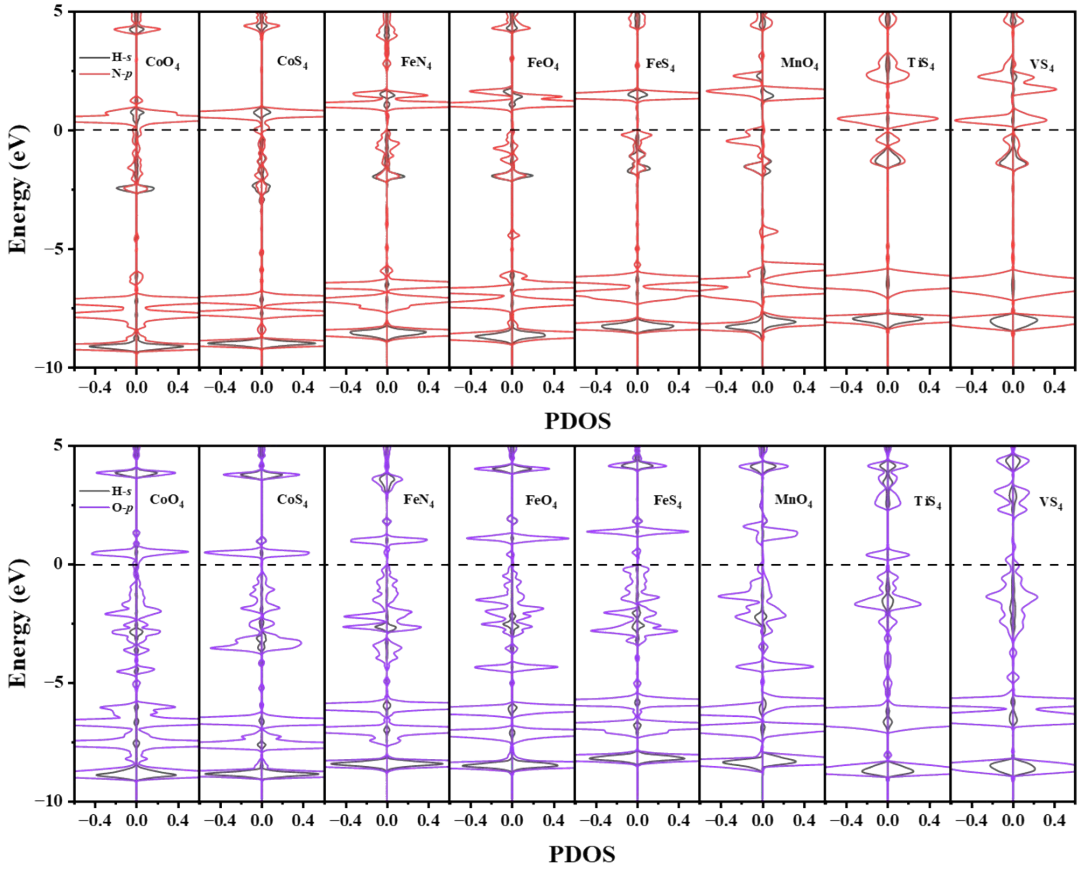

Fig. S13 PDOS of MnO_4-HTP adsorbed with HNO and NOH. The Fermi level is set to 0 eV.

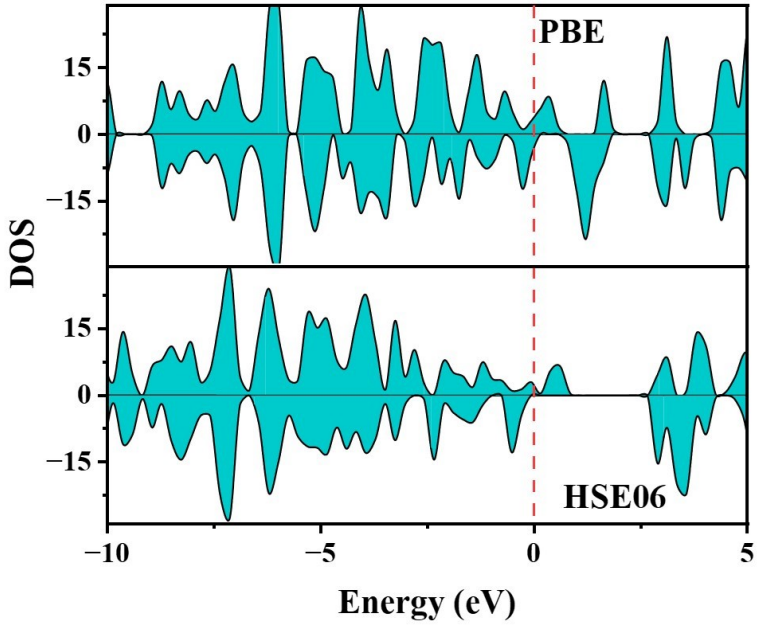

Fig. S14 The PBE functional and Heyd-Scuseria-Ernzerhof (HSE06) hybrid functional are adopted to calculate the PDOS of MnO_4-HTP.

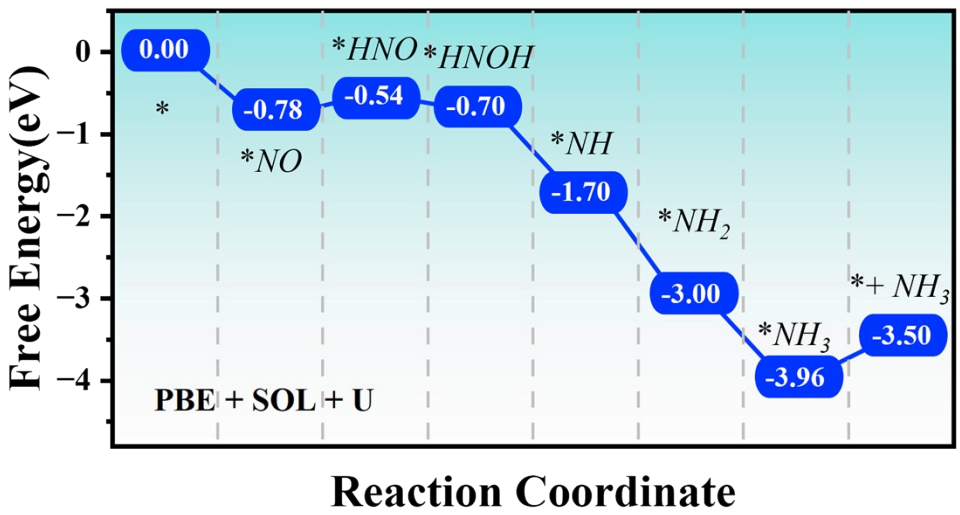

Fig. S15 Free energy diagrams of electrochemical NO-to-NH_3 conversion on MnO_4-HTP by PBE+SOL+U.

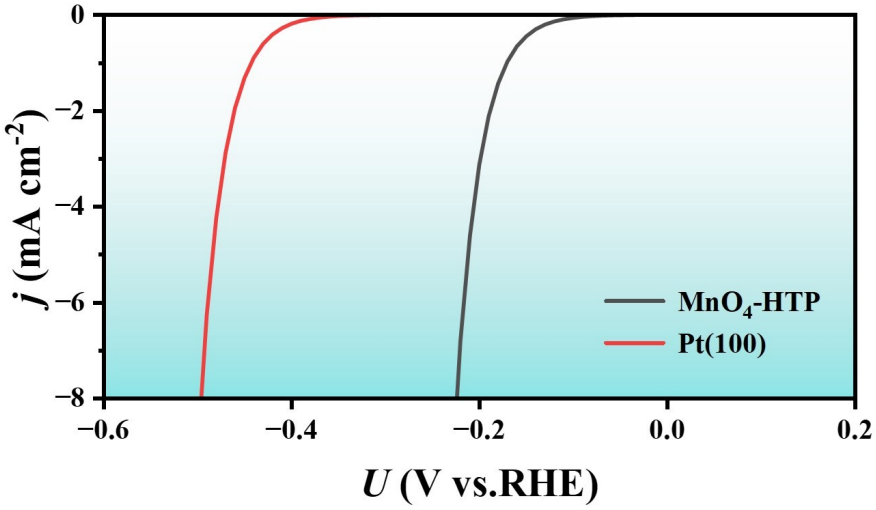

Fig. S16 Simulated polarization curve of MnO_4-HTP and Pt (100).

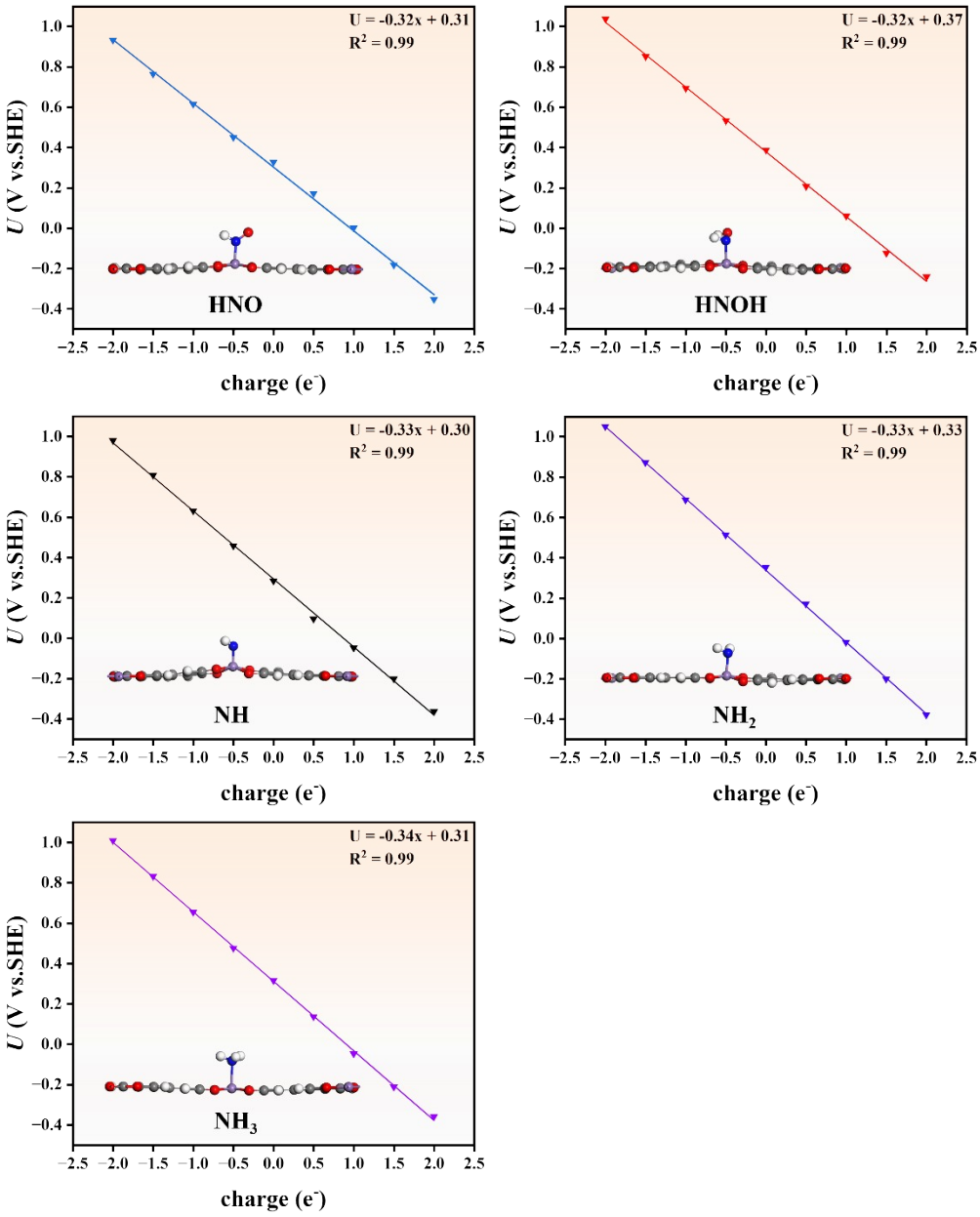

Fig. S17 Total energies of *HNO, *HNOH, *NH, *NH_2 and *NH_3 as a function of applied potential U. The calculated total energy is represented by triangles, and the fitting data is represented by solid lines.

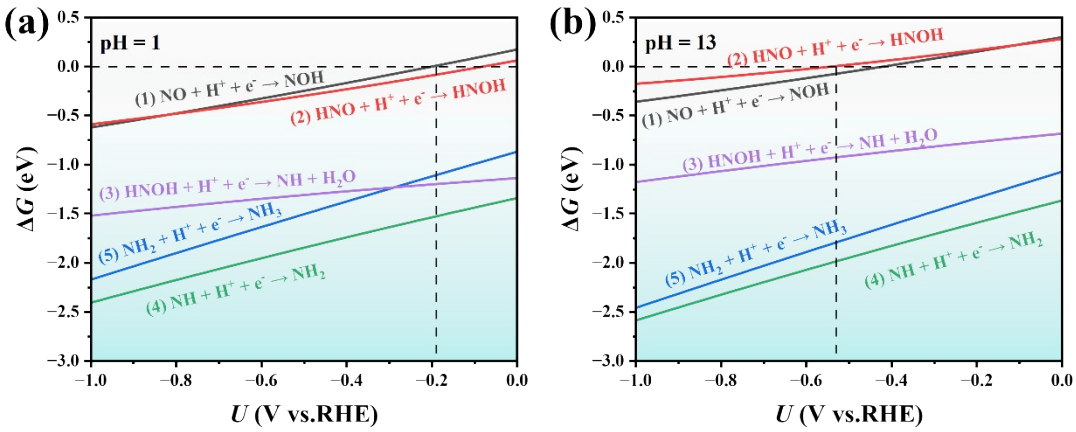

Fig. S18 The free energy curves of MnO_4-HTP under varying electrode potentials at (a) pH=1, and (b) pH=13.

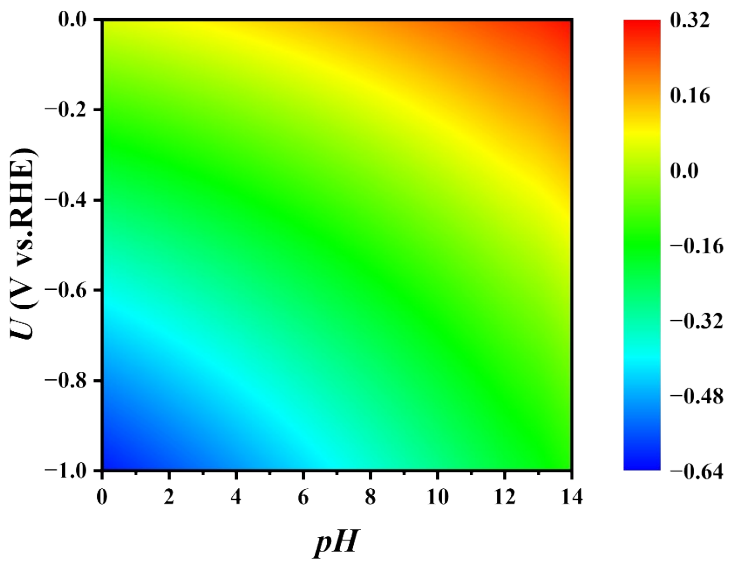

Fig. S19 pH-dependent and potential-dependent contour plot of the reaction energy for the second protonation step.

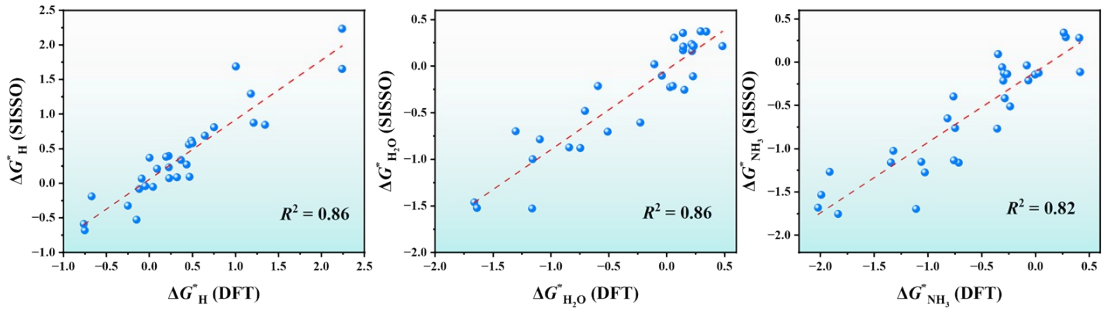

Fig. S20 The DFT-calculated ΔG_{*H}, ΔG_{*H2O} and ΔG_{*NH3} values of TMX_4-HTP were compared with the SISSO predicted values.

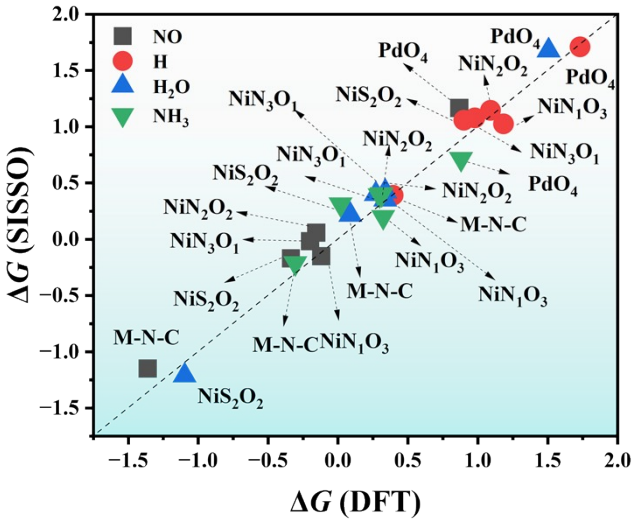

Fig S21 Comparison of DFT-calculated ΔG_{*H}, ΔG_{*H2O} and ΔG_{*NH3} values with the SISSO-predicted values.

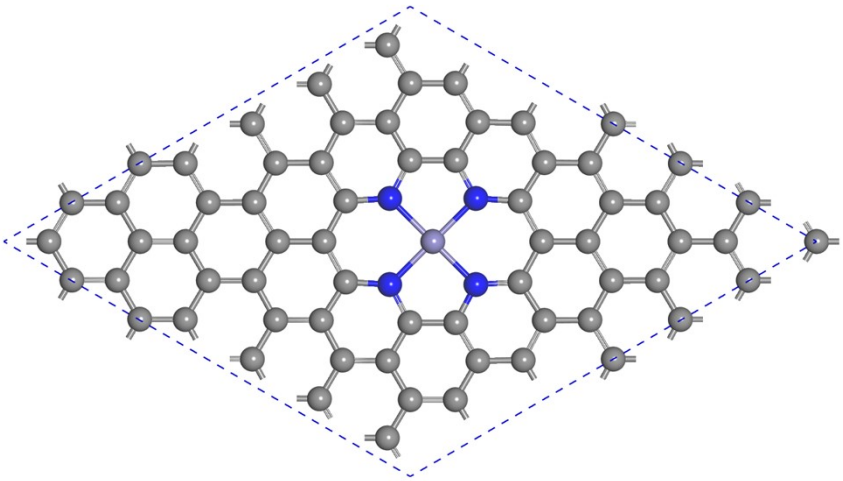

Fig. S22 The structure of Fe–N–C. The Fe–N–C SAC was modeled by a FeN_4 site embedded into a monolayer graphene in an orthorhombic cell with the lattice parameter of a = 15.16 Å and b = 20 Å.

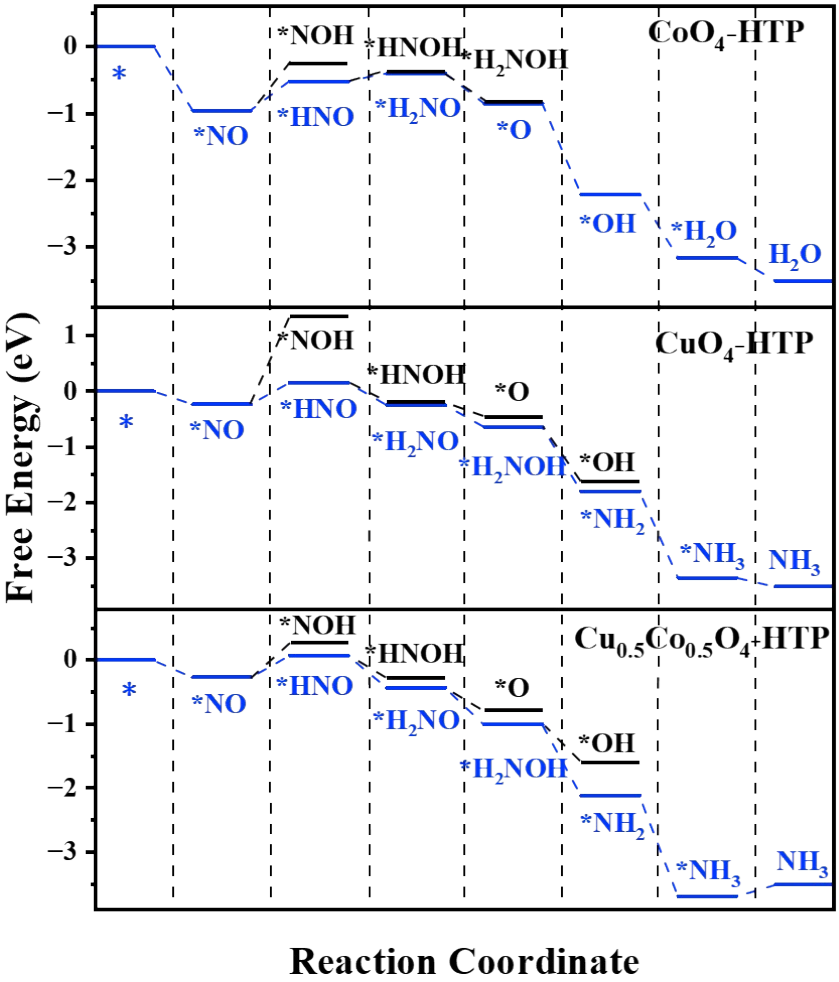

Fig. S23 Free energy diagrams of electrochemical NO-to-NH_3 conversion on CoO_4-HTP, CuO_4-HTP and $Cu_{0.5}Co_{0.5}O_4$-HTP.

Tab. S1: Calculated energies of MnO_4-HTP at different vacuum spaces, using the energy of MnO_4-HTP at a 12 Å vacuum space as the reference.

Vacuum space (Å)	ΔE_{*NO} (eV)	ΔE_{*HNO} (eV)
12	0.00	0.00
15	0.00	0.02
20	0.00	0.02
30	-0.01	0.00

Tab. S2 TMX_4-HTP energy and lattice length a, b

TMN_4-HTP	Energy (eV)	a = b (Å)	TMO_4-HTP	Energy (eV)	a = b (Å)
Sc	–540.60	22.88	Sc	–480.37	22.37
Ti	–542.85	22.47	Ti	–482.29	22.02
V	–543.24	22.39	V	–481.94	21.91
Cr	–544.50	22.23	Cr	–480.77	21.84
Mn	–543.62	22.16	Mn	–479.86	21.71
Fe	–539.41	22.02	Fe	–474.16	21.63
Co	–535.84	21.86	Co	–469.20	21.45
Ni	–530.91	21.85	Ni	–464.51	21.44
TMP_4-HTP	Energy (eV)	a = b (Å)	TMS_4-HTP	Energy (eV)	a = b (Å)
Sc	–489.84	25.43	Sc	–444.02	24.25
Ti	–493.00	24.96	Ti	–446.77	23.89
V	–494.91	24.52	V	–447.32	23.75
Cr	–496.60	24.32	Cr	–448.77	23.57
Mn	–496.98	24.14	Mn	–448.36	23.49
Fe	–494.79	23.99	Fe	–445.06	23.34
Co	–490.79	23.87	Co	–441.46	23.19
Ni	–487.44	23.76	Ni	–437.26	23.15

Tab. S3 Computed the total energy of a metal atom in its most stable bulk structure (μ_{TM}), formation energy (E_f), standard dissolution potential (U°_{diss}) of metal atoms, the number of transferred electrons (Ne) during the dissolution, and dissolution potential (U_{diss}) of metals.

TMN_4-HTP	μ_{TM} (eV)	E_f (eV)	U°_{diss} (V)	N_e	U_{diss} (V)
Sc	–6.34	–7.75	–2.08	3	0.50
Ti	–7.9	–6.94	–1.63	2	1.84
V	–9.09	–5.88	–1.18	2	1.76
Cr	–9.64	–5.75	–0.91	2	1.97
Mn	–9.16	–5.94	–1.19	2	1.78
Fe	–8.46	–5.24	–0.45	2	2.17
Co	–7.11	–5.23	–0.28	2	2.33
Ni	–5.78	–5.08	–0.26	2	2.28
TMO_4-HTP	μ_{TM} (eV)	E_f (eV)	U°_{diss} (V)	N_e	U_{diss} (V)
Sc	–6.34	–9.09	–2.08	3	0.95
Ti	–7.9	–8.17	–1.63	2	2.45
V	–9.09	–6.86	–1.18	2	2.25
Cr	–9.64	–5.92	–0.91	2	2.05
Mn	–9.16	–6.10	–1.19	2	1.86
Fe	–8.46	–4.90	–0.45	2	2.00
Co	–7.11	–4.59	–0.28	2	2.02
Ni	–5.78	–4.36	–0.26	2	1.92
TMP_4-HTP	μ_{TM} (eV)	E_f (eV)	U°_{diss} (V)	N_e	U_{diss} (V)
Sc	–6.34	–3.68	–2.08	3	–0.85
Ti	–7.9	–3.17	–1.63	2	–0.04
V	–9.09	–2.62	–1.18	2	0.13
Cr	–9.64	–2.63	–0.91	2	0.41
Mn	–9.16	–3.24	–1.19	2	0.43
Fe	–8.46	–3.21	–0.45	2	1.16
Co	–7.11	–3.23	–0.28	2	1.34
Ni	–5.78	–3.34	–0.26	2	1.41
TMS_4-HTP	μ_{TM} (eV)	E_f (eV)	U°_{diss} (V)	N_e	U_{diss} (V)
Sc	–6.34	–6.80	–2.08	3	0.19
Ti	–7.9	–6.16	–1.63	2	1.45
V	–9.09	–5.15	–1.18	2	1.39
Cr	–9.64	–5.08	–0.91	2	1.63
Mn	–9.16	–5.43	–1.19	2	1.52
Fe	–8.46	–5.03	–0.45	2	2.06
Co	–7.11	–5.17	–0.28	2	2.31
Ni	–5.78	–5.11	–0.26	2	2.29

Tab. S4 Free energies of NO on TMX_4-HTPs with N-end, O-end, and side-on patterns, the lowest energies are highlighted in red.

TMN_4-HTP	N-end (eV)	O-end (eV)	side-on (eV)	TMO_4-HTP	N-end (eV)	O-end (eV)	side-on (eV)
Sc	–1.47	–0.63	NAN	Sc	–1.01	–0.67	NAN
Ti	–2.38	–0.96	–1.28	Ti	–1.70	–1.29	–1.41
V	–2.09	–0.84	–1.58	V	–1.52	–0.31	–0.96
Cr	–1.69	–0.10	–0.76	Cr	–1.49	0.01	–0.65
Mn	–1.20	0.35	–0.30	Mn	–0.78	NAN	NAN
Fe	–1.23	0.28	NAN	Fe	–0.97	0.23	NAN
Co	–0.73	0.43	NAN	Co	–0.96	0.12	NAN
Ni	0.07	0.65	NAN	Ni	–0.21	NAN	NAN
TMP_4-HTP	N-end (eV)	O-end (eV)	side-on (eV)	TMS_4-HTP	N-end (eV)	O-end (eV)	side-on (eV)
Sc	NAN	NAN	NAN	Sc	–0.86	–0.17	NAN
Ti	NAN	NAN	NAN	Ti	–2.29	–1.42	NAN
V	–3.59	–1.26	–2.67	V	–2.35	–1.24	–1.51
Cr	–2.75	–0.73	–1.61	Cr	–1.71	–0.05	NAN
Mn	–2.15	–0.17	–0.79	Mn	–1.44	0.42	–0.69
Fe	–2.00	–0.09	NAN	Fe	–1.39	0.44	–0.19
Co	–2.22	NAN	NAN	Co	–0.78	0.30	NAN
Ni	–0.88	–0.87	–0.67	Ni	–0.09	NAN	NAN

Tab. S5 Free energies of NO (ΔG_{*NO}), H (ΔG_{*H}), H2O molecules (ΔG_{*H2O}), and NH3 molecules (ΔG_{*NH3}) on TMX_4-HTPs, the lowest energies are highlighted in red.

TMN_4-HTP	ΔG_{*NO}	ΔG_{*H}	ΔG_{*H2O}	ΔG_{*NH3}
Sc	–1.47	2.24	–0.74	–0.71
Ti	–2.38	–0.09	–1.16	–1.11
V	–2.09	0.04	–0.51	–1.03
Cr	–1.69	0.23	0.23	–0.35
Mn	–1.20	0.46	0.22	0.00
Fe	–1.23	0.22	0.23	–0.06
Co	–0.73	0.43	0.22	0.42
Ni	NAN	NAN	NAN	NAN
TMO_4-HTP	ΔG_{*NO}	ΔG_{*H}	ΔG_{*H2O}	ΔG_{*NH3}
Sc	–1.01	2.24	–1.09	–1.32
Ti	–1.70	0.00	–1.66	–1.99
V	–1.52	0.09	–0.23	–0.76
Cr	–1.49	0.37	–0.11	–0.82
Mn	–0.78	1.35	0.07	–0.31
Fe	–0.97	0.65	0.14	–0.29
Co	–0.96	0.49	0.34	–0.08
Ni	–0.21	1.18	0.29	0.26
TMP_4-HTP	ΔG_{*NO}	ΔG_{*H}	ΔG_{*H2O}	ΔG_{*NH3}
Sc	NAN	NAN	NAN	NAN
Ti	NAN	NAN	NAN	NAN
V	–3.59	–0.75	–1.16	–1.83
Cr	–2.75	–0.15	–0.71	–1.34
Mn	–2.15	–0.12	0.15	–0.28
Fe	–2.00	–0.25	0.03	–0.23
Co	–2.22	–0.76	–0.59	–0.76
Ni	–0.88	–0.67	0.05	–0.35
TMS_4-HTP	ΔG_{*NO}	ΔG_{*H}	ΔG_{*H2O}	ΔG_{*NH3}
Sc	–0.86	1.01	–0.84	–1.06
Ti	–2.29	0.47	–1.64	–2.02
V	–2.35	–0.05	–1.30	–1.91
Cr	–1.71	0.32	–0.04	–0.75
Mn	–1.44	0.50	0.14	–0.26
Fe	–1.39	0.20	0.14	–0.30
Co	–0.78	0.23	0.48	0.03
Ni	–0.09	0.75	0.23	0.41

Tab. S6 Energy(ΔG_1) required for the first protonation step of NO + H + e^- → HNO(NOH), those with $\Delta G_1 < 0.5$ eV are highlighted in red.

TMN_4-HTP	ΔG_1	TMO_4-HTP	ΔG_1
Sc	–0.24	Sc	NAN
Ti	0.16	Ti	NAN
V	0.53	V	0.27
Cr	0.86	Cr	1.86
Mn	0.54	Mn	0.21
Fe	0.30	Fe	0.32
Co	0.55	Co	0.43
Ni	NAN	Ni	0.55
TMP_4-HTP	ΔG_1	TMS_4-HTP	ΔG_1
Sc	NAN	Sc	NAN
Ti	NAN	Ti	0.43
V	1.00	V	0.34
Cr	1.01	Cr	0.63
Mn	1.17	Mn	0.80
Fe	0.92	Fe	0.40
Co	0.78	Co	0.42
Ni	0.30	Ni	0.52

Tab. S7 The energy of all the possible intermediates, and the free energy of the five hydrogenation steps.

ScN_4-HTP	adsorbate	Energy (eV)	Free energy (eV)
	slab	–540.60	
step0	*N_O	–554.80	–1.47
step1	*HN_O	–558.79	–0.24
	*N_OH	–557.41	1.00
step2	*2HN_O	–563.43	–0.83
	*HN_OH	–562.54	0.01
step3	*2HN_OH	–566.04	1.07
	*O	–546.43	0.57
step4	*OH	–552.52	–2.43
step5	*H_2O	–556.10	0.15
step6	H_2O	–540.60	0.74
TiN_4-HTP	adsorbate	Energy (eV)	Free energy (eV)
	slab	–542.85	
step0	*N_O	–558.02	–2.38
step1	*HN_O	–561.53	0.16
	*N_OH	–561.18	0.55
step2	*2HN_O	–566.39	–0.95
	*HN_OH	–565.50	–0.18
step3	*2HN_OH	–568.71	1.27
	*O	–549.94	–0.06
step4	*OH	–555.69	–2.09
step5	*H_2O	–558.85	0.66
step6	H_2O	–542.85	1.16
FeN_4-HTP	adsorbate	Energy (eV)	Free energy (eV)
	slab	–539.41	
step0	*N_O	–553.50	–1.23
step1	*HN_O	–556.93	0.30
	*N_OH	–556.28	0.94
step2	*2HN_O	–560.25	0.39
	*HN_OH	–560.31	0.36
step3	*2HN_OH	–564.07	0.09
	*NH	–550.00	–1.19
step4	*NH_2	–555.07	–1.06
step5	*NH_3	–559.55	–0.75
step6	NH_3	–539.41	0.06
VO_4-HTP	adsorbate	Energy (eV)	Free energy (eV)
	slab	–481.94	
step0	*N_O	–496.29	–1.52
step1	*HN_O	–499.71	0.27

	*N_OH	–499.52	0.46
step2	*2HN_O	–504.72	–1.13
	*HN_OH	–504.10	–0.60
step3	*2HN_OH	–507.55	0.81
	*O	–489.86	–1.60
step4	*OH	–493.87	–0.27
step5	*H_2O	–497.03	0.52
step6	H_2O	–481.94	0.23
MnO_4-HTP	adsorbate	Energy (eV)	Free energy (eV)
	slab	–479.86	
step0	*N_O	–493.48	–0.78
step1	*HN_O	–496.98	0.21
	*N_OH	–496.44	0.75
step2	*2HN_O	–499.66	1.06
	*HN_OH	–500.57	0.15
step3	*2HN_OH	–504.90	–0.58
	*NH	–490.26	–0.90
step4	*NH_2	–495.43	–1.41
step5	*NH_3	–500.27	–1.08
step6	NH_3	–479.86	0.31
FeO_4-HTP	adsorbate	Energy (eV)	Free energy (eV)
	slab	–474.16	
step0	*N_O	–487.99	–0.97
step1	*HN_O	–491.38	0.32
	*N_OH	–490.79	0.90
step2	*2HN_O	–494.83	0.23
	*HN_OH	–494.64	0.45
step3	*2HN_OH	–499.16	–0.80
	*O	–479.45	–0.94
step4	*OH	–484.37	–1.15
step5	*H_2O	–488.82	–0.85
step6	H_2O	–474.16	–0.14
CoO_4-HTP	adsorbate	Energy (eV)	Free energy (eV)
	slab	–469.20	
step0	*N_O	–482.99	–0.96
step1	*HN_O	–486.29	0.43
	*N_OH	–485.51	1.21
step2	*2HN_O	–489.92	0.12
	*HN_OH	–489.86	0.15
step3	*2HN_OH	–494.06	–0.42
	*O	–473.97	–0.45
step4	*OH	–479.13	–1.36
step5	*H_2O	–483.67	–0.95

step6	H_2O	–469.20	–0.34
NiP_4-HTP	adsorbate	Energy (eV)	Free energy (eV)
	slab	–487.44	
step0	*N_O	–501.16	–0.88
step1	*HN_O	–503.72	1.14
	*N_OH	–504.56	0.28
step2	*2HN_O	–508.10	0.25
	*HN_OH	–508.35	0.04
step3	*2HN_OH	–512.79	–0.91
	*NH	–499.73	–2.74
step4	*NH_2	–502.79	0.59
step5	*NH_3	–507.90	–1.35
step6	NH_3	–487.44	0.35
TiS_4-HTP	adsorbate	Energy (eV)	Free energy (eV)
	slab	–446.77	
step0	*N_O	–461.79	–2.29
step1	*HN_O	–465.16	0.43
	*N_OH	–464.89	0.73
step2	*2HN_O	–470.14	–1.23
	*HN_OH	–469.39	–0.45
step3	*2HN_OH	–473.57	0.35
	*O	–454.79	–1.00
step4	*OH	–459.41	–0.99
step5	*H_2O	–463.24	–0.05
step6	H_2O	–446.77	1.64
VS_4-HTP	adsorbate	Energy (eV)	Free energy (eV)
	slab	–447.32	
step0	*N_O	–462.51	–2.35
step1	*HN_O	–465.84	0.35
	*N_OH	–465.72	0.48
step2	*2HN_O	–470.85	–1.13
	*HN_OH	–470.07	–0.44
step3	*2HN_OH	–474.00	0.52
	*O	–455.77	–1.38
step4	*OH	–459.67	–0.24
step5	*H_2O	–463.48	–0.05
step6	H_2O	–447.32	1.30
FeS_4-HTP	adsorbate	Energy (eV)	Free energy (eV)
	slab	–445.06	
step0	*N_O	–459.32	–1.39
step1	*HN_O	–462.54	0.47
	*N_OH	–461.93	1.09
step2	*2HN_O	–465.81	0.46

	*HN_OH	–465.90	0.39
step3	*2HN_OH	–470.10	–0.51
	*NH	–455.61	–0.93
step4	*NH_2	–460.71	–1.30
step5	*NH_3	–465.44	–1.03
step6	NH_3	–445.06	0.30
CoS_4-HTP	adsorbate	Energy (eV)	Free energy (eV)
	slab	–441.46	
step0	*N_O	–455.03	–0.78
step1	*HN_O	–458.37	0.42
	*N_OH	–457.71	1.08
step2	*2HN_O	–461.94	0.15
	*HN_OH	–461.74	0.37
step3	*2HN_OH	–466.17	–0.43
	*O	–446.20	–0.62
step4	*OH	–451.10	–1.17
step5	*H_2O	–455.76	–1.02
step6	H_2O	–441.46	–0.48

Tab. S8 Transfer charge of TM atoms, and the N-O bond of adsorbed NO on TMX_4-HTPs.

TMN_4-HTP	Translate charge (e^-)	N-O bond (Å)	TMO_4-HTP	Translate charge (e^-)	N-O bond (Å)
Sc	0.40348	1.19808	Sc	0.26167	1.18518
Ti	0.50708	1.20156	Ti	0.41017	1.19433
V	0.44967	1.20008	V	0.30807	1.19106
Cr	0.43873	1.1995	Cr	0.29874	1.18734
Mn	0.34409	1.1906	Mn	0.15188	1.1784
Fe	0.38448	1.19437	Fe	0.23941	1.18434
Co	0.18459	1.18634	Co	0.17147	1.18179
Ni	NAN	NAN	Ni	0.08413	1.17775
TMP_4-HTP	Translate charge (e^-)	N-O bond (Å)	TMS_4-HTP	Translate charge (e^-)	N-O bond (Å)
Sc	NAN	NAN	Sc	0.22112	1.17567
Ti	NAN	NAN	Ti	0.32804	1.1829
V	0.48947	1.19306	V	0.35708	1.18548
Cr	0.42713	1.18901	Cr	0.3021	1.18283
Mn	0.26618	1.17993	Mn	0.28027	1.18199
Fe	0.18829	1.17966	Fe	0.22167	1.18116
Co	0.36646	1.18601	Co	0.1449	1.17477
Ni	0.16625	1.17638	Ni	0.04461	1.17103

Tab. S9 Adsorption free energies of HNO ($\Delta^{*}G_{HNO}$), NOH (ΔG_{*NOH}), $\Delta G_{HNO}-\Delta G_{NOH}$, the lowest energies are highlighted in red.

TMN_4-HTP	ΔG_{*HNO} (eV)	ΔG_{*NOH} (eV)	$\Delta G_{*HNO}-\Delta G_{*NOH}$ (eV)	TMO_4-HTP	ΔG_{*HNO} (eV)	ΔG_{*NOH} (eV)	$\Delta G_{*HNO}-\Delta G_{*NOH}$ (eV)
Sc	–1.72	–0.34	–1.38	Sc	NAN	NAN	NAN
Ti	–2.22	–1.87	–0.35	Ti	NAN	NAN	NAN
V	–1.56	–1.47	–0.09	V	–1.25	–1.06	–0.19
Cr	–0.18	–0.82	0.64	Cr	0.37	0.68	–0.31
Mn	–0.66	–0.09	–0.57	Mn	–0.57	–0.02	–0.54
Fe	–0.93	–0.28	–0.65	Fe	–0.65	–0.05	–0.59
Co	–0.18	0.63	–0.81	Co	–0.52	0.26	–0.78
Ni	NAN	NAN	NAN	Ni	0.34	1.12	–0.77
TMP_4-HTP	ΔG_{HNO} (eV)	ΔG_{NOH} (eV)	$\Delta G_{HNO}-\Delta G_{NOH}$ (eV)	TMS_4-HTP	ΔG_{HNO} (eV)	ΔG_{NOH} (eV)	$\Delta G_{HNO}-\Delta G_{NOH}$ (eV)
Sc	NAN	NAN	NAN	Sc	NAN	NAN	NAN
Ti	NAN	NAN	NAN	Ti	–1.86	–1.60	–0.27
V	–2.27	–2.58	0.31	V	–2.01	–1.88	–0.13
Cr	–1.59	–1.74	0.15	Cr	–1.08	–1.07	–0.01
Mn	–0.97	–0.80	–0.17	Mn	–0.64	–0.32	–0.31
Fe	–1.08	–0.46	–0.62	Fe	–0.99	–0.38	–0.61
Co	–1.43	–0.84	–0.60	Co	–0.36	0.30	–0.66
Ni	–0.58	0.26	–0.84	Ni	0.43	1.69	–1.26

Tab. S10 Charge transfer of X atoms (Q_X) before reaction, number of valence electrons (N), atomic radius (AR), ion radius (IR), first ionization energy (IE), electron affinity of the metal atom (EA), density of TM (ρ_{TM}), relative atomic mass (M), pauling electronegativity (χ) of each investigated TMX_4-HTPs.

Materials	Q_X	N	AR	IR	IE	EA	ρ_{TM}	M	χ
ScN	25.33405	3	144	74.5	633	–18	2.99	44.95591	1.36
TiN	25.21795	4	136	86	659	–8	4.51	47.867	1.54
VN	25.0772	5	125	79	651	–51	6.11	50.9415	1.63
CrN	24.82608	6	127	80	653	–64	7.14	51.9961	1.66
MnN	24.69297	7	139	67	717	0	7.47	54.93805	1.55
FeN	24.64825	6	125	78	763	–16	7.87	55.845	1.83
CoN	24.6003	4	126	74.5	760	–64	8.9	58.9332	1.88
NiN	24.59735	4	121	69	737	–112	8.91	58.6934	1.91
VP	17.53348	5	125	79	651	–51	6.11	50.9415	1.63
CrP	17.2083	6	127	80	653	–64	7.14	51.9961	1.66
MnP	16.91967	7	139	67	717	0	7.47	54.93805	1.55
FeP	16.62054	6	125	78	763	–16	7.87	55.845	1.83
CoP	16.54063	4	126	74.5	760	–64	8.9	58.9332	1.88
NiP	16.48769	4	121	69	737	–112	8.91	58.6934	1.91
ScO	28.57744	3	144	74.5	633	–18	2.99	44.95591	1.36
TiO	28.34883	4	136	86	659	–8	4.51	47.867	1.54
VO	28.20933	5	125	79	651	–51	6.11	50.9415	1.63
CrO	28.19818	6	127	80	653	–64	7.14	51.9961	1.66
MnO	28.12737	7	139	67	717	0	7.47	54.93805	1.55
FeO	27.93121	6	125	78	763	–16	7.87	55.845	1.83
CoO	27.83559	4	126	74.5	760	–64	8.9	58.9332	1.88
NiO	27.80528	4	121	69	737	–112	8.91	58.6934	1.91
ScS	25.53636	3	144	74.5	633	–18	2.99	44.95591	1.36
TiS	25.47583	4	136	86	659	–8	4.51	47.867	1.54
VS	25.20713	5	125	79	651	–51	6.11	50.9415	1.63
CrS	25.00778	6	127	80	653	–64	7.14	51.9961	1.66
MnS	24.90353	7	139	67	717	0	7.47	54.93805	1.55
FeS	24.51769	6	125	78	763	–16	7.87	55.845	1.83
CoS	24.21995	4	126	74.5	760	–64	8.9	58.9332	1.88
NiS	24.1118	4	121	69	737	–112	8.91	58.6934	1.91

References

1. J. é. Filhol and M. Neurock, *Angewandte Chemie*, 2010, **45**, 402-406.

2. R. Ouyang, E. Ahmetcik, C. Carbogno, M. Scheffler and L. M. Ghiringhelli, *Journal of Physics: Materials*, 2019, **2**.

3. R. Ouyang, S. Curtarolo, E. Ahmetcik, M. Scheffler and L. M. Ghiringhelli, *Physical Review Materials*, 2018, **2**.